Received: 13 September 2019 | Revised: 10 December 2019 | Accepted: 22 December 2019

DOI: 10.1002/eom2.12012

RESEARCH ARTICLE

EcoMat FUNCTIONAL MATERIALS FOR GREEN ENERGY AND ENVIRONMENT WILEY

Reversible ternary nickel-cobalt-iron catalysts for intermittent water electrolysis

Xunyu Lu[1] | **Qingran Zhang**[2] | **Yun Hau Ng**[3] | **Chuan Zhao**[1]

[1]School of Chemistry, The University of New South Wales, Sydney, New South Wales, Australia

[2]Particles and Catalysis Research Group, School of Chemical Engineering, The University of New South Wales, Sydney, New South Wales, Australia

[3]School of Energy and Environment, City University of Hong Kong, Tat Chee Avenue Kowloon, Hong Kong

Correspondence
Chuan Zhao, School of Chemistry, The University of New South Wales, Sydney, NSW 2052, Australia.
Email: chuan.zhao@unsw.edu.au

Present address
Xunyu Lu, School of Chemical Engineering, The University of New South Wales, Sydney, NSW 2052, Australia

Funding information
Australian Research Council, Grant/Award Number: DP160103107

Abstract

Global-scale application of water splitting technology for hydrogen fuel production and storage of intermittent renewable energy sources such as solar and wind has called for the development of oxygen evolution catalysts and hydrogen evolution catalysts that are inexpensive, efficient, robust, and can withstand frequent power interruptions and shutdowns. Current water electrolyzers must operate with a protective current in stand-by/idle modes to avoid a substantial catalyst degradation. Here, we show a hierarchically structured porous ternary composite catalyst of nickel, cobalt and iron (NiCoFe) hydroxides prepared via electrodeposition on three-dimensional (3D) nickel foam (NF) substrates as reversible bifunctional electrodes for both oxygen evolution reaction (OER) and hydrogen evolution reaction (HER). The NiCoFe/NF electrode exhibits exceptionally high catalytic activity, requiring overpotentials as low as 220 and 50 mV, respectively, for OER and HER to occur. In a water electrolysis cell comprising of two NiCoFe/NF electrodes, an overall cell overpotential of merely 300 mV is required to deliver a stabilized current density of 3 mA cm^{-2}. The ternary electrocatalyst also exhibits prolonged stability under both continuous and intermittent electrolysis and can be used for oxygen evolution and hydrogen evolution reversibly without degradation.

KEYWORDS

bifunctional, electrodeposition, nickel-cobalt-iron, reversible electrolyzer, water splitting

1 | INTRODUCTION

The increasing demands for clean energy have triggered tremendous research interest in electrochemical energy conversion and storage systems with minimum environmental impact. Electrolytic splitting of water has attracted intensive research interests and is considered as the "simplest" and "cleanest" method to store electricity generated by renewable energy resources, for example, solar and wind, into high purity hydrogen fuels.[1-3] Nevertheless, global-scale application of electrolytic water splitting has been constrained by (a) high energy consumption, owing to the sluggish kinetics and high overpotentials of the two half reactions, oxygen evolution reactions (OERs) and hydrogen evolution reactions (HERs) and (b) high cost, attributed largely to the use of precious metal catalysts, such as oxides of ruthenium and iridium for OER,[4-6] and platinum for HER.[7,8]

Therefore, the development of earth abundant material-based catalysts with high efficiency and stability is key to global-scale utilization of the water splitting technology.

For industrial application of water splitting, using the same electrode for both OER and HER can remove the problems with catalyst contamination and membrane separators, thus can significantly improve the integration and simplification of the water splitting system and lowering the manufacturing cost of produced hydrogen. Nevertheless, the design of bifunctional electrodes that are active and stable toward both OER and HER in the same electrolytes (either strongly acidic or strongly alkaline) remains challenging for most of the Earth-abundant materials and has been scarcely studied.[9-12] Furthermore, for practical applications, the OER and HER catalysts need not only to have prolonged stability, but also to withstand frequent power interruptions during cell shutdowns. It is known that during power interruptions (ie, when no power is provided by renewable energy sources), a reverse current takes place in water electrolyzer from anode to cathode through bipolar plate, and degrades the electrodes by the reduction of the anode and/or oxidation of the cathode, resulting in compositional as well as structural change and eventually catalyst deactivation.[13-15] This is particularly important for storage of electricity generated from renewable resources such as solar and wind because these energy sources are intermittent and power interruptions are almost inevitable. However, most of catalysts reported to date are stable under continuous operation conditions, only a few can stand frequent power shutdowns while maintaining high activity and stability.

Extensive recent research interests have been focusing on using low cost first row transition metals such as Ni and Co for water splitting because of their excellent activity and stability.[1,16-18] However, only limited amount of reported catalysts are able to achieve the high activity and stability matching those of RuO_2, IrO_2, and Pt, particularly under harsh working conditions required in industrial applications such as high current density and strong gas evolution. In this regards, multimetallic composites containing two or more metal components can exhibit enhanced electrochemical performances due to the synergistic metal-metal interactions, and also offer the flexibility to satisfy specific applications by adjusting the alloy compositions. Incorporation of iron (Fe) into nickel or cobalt, either as impurities or components, generates strong synergistic effects, resulting in significantly more active binary OER catalysts than either Ni or Co alone,[19-29] with some even outperforming the benchmark Ir-based catalysts. The combination of Ni and Co also leads to a substantial enhancement in the catalytic activity of HER.[30,31] However, a ternary nickel-cobalt-iron catalyst that is active and stable for reversible OER and HER has been rarely studied. Furthermore, the interdependence of the electrochemical performances of these multimetallic catalysts upon the compositions is yet to be understood and remains an intriguing area to explore.

In this study, we report a simple electrodeposition method for preparing a hierarchical porous catalyst containing an extremely thin layer of amorphous hydroxide of Fe, Ni, and Co onto macroporous nickel foam (NiCoFe/NF) for robust continuous and intermittent water splitting. Ternary NiCoFe alloy films owing to their interesting magnetic and magnetoresistance properties have attracting attentions for use in computer read/write heads and microelectromechanical systems in magnetic recording industry.[32] Recent studies also report promising OER performance for amorphous metal oxide films containing Fe, Co, and Ni,[19,23,33] Nevertheless, the catalytic property of NiFeCo composites for HER is still unsatisfactory. Here, we prepare a bifunctional NiCoFe/NF electrode that is highly active toward both OER and HER in strongly alkaline media, requiring overpotentials only of 240 and 95 mV, respectively, to deliver a current density of 10 mA cm^{-2}. Remarkably, the NiCoFe/NF electrode is highly reversible and can be switched between OER and HER during electrolysis with prominent stability and robustness under frequent shutdown conditions.

2 | RESULTS

2.1 | Electrodeposition and physical characterizations

Electrodeposition is a versatile and scalable industrial process and can afford optimal adherence of the active catalysts to the underlying nickel substrate without using any insulating chemical binders, thereby offering excellent mechanical robustness and lowering the overpotential introduced by ohmic loss.[34] NF is selected as the catalyst support owing to its unique three-dimensional (3D) interconnected porous structure, which offers large accessible electroactive surface area inside its 3D skeleton.[35,36] Furthermore, its extra-large pores (>200 μm) allows for fast mass transport and dissipation of gaseous bubbles having sizes from tens to hundreds of microns, reducing significantly the "bubble overpotentials," one of the main cause of energy loss especially at high current densities.[37,38] Different from conventional electrodeposition method where Ni, Fe, and Co ions are directly reduced and deposited onto the substrate to form thick films,[23,32,33] we adapted here an indirect deposition approach for preparation of extremely thin NiFeCo hydroxide composite with unique mesoporous nanoflake/nanosheet morphologies. The

electrodeposition was performed in an electrolyte containing nickel (II), cobalt (II), and/or iron (III) nitrates using NF as the working electrode. Upon the application of a deposition potential at −1.0 V vs Ag/AgCl, the nitrate ions are reduced to OH^- ions and increase the local pH value (Equation 1). The OH^- ions then reacted with the Ni^{2+}, Co^{2+}, and/or Fe^{3+} forming bimetallic or trimetallic hydroxide composites on the surface of NF (Equation 2, see details in Methods).[32,39,40] Figure 1A shows the scanning electron microscopy (SEM) image of the NiCo bimetallic composite deposited on nickel foam (NiCo/NF) from the electrolyte containing equal molar (2.5 mM) of Ni^{2+} and Co^{2+}. The macroscopic 3D structure of NF enables a full utilization of its interior area, offering a larger surface area than other commonly used substrates such as carbon paper, titanium plate, and conductive glasses. A thin film of the composite is uniformly deposited onto the 3D skeleton of NF without blocking the pores. Figure 1B displays the high magnification SEM image of the small area selected in Figure 1A. The deposited NiCo film exhibits a nanoporous structure with highly curved and rippled, but interconnected nanoflakes/nanosheets. The nanopores have sizes ranging from 100-200 nm, which is known to enhance the contact between electrolytes and the active catalysts surface area.[40] Incorporating of iron into the NiCo composite induces no significant morphological change of the deposits on NF.

Figure 1C,D represent the SEM images of the trimetallic NiCoFe composites deposited on NF from the electrolyte containing equal molar (1.67 mM) of Ni^{2+}, Co^{2+}, and Fe^{3+} (hereafter mentioned as NiCoFe/NF). The NiCoFe is also deposited uniformly on the NF, forming highly curved and rippled nanoflakes (Figure 1D), which resembles the NiCo. We further carried out a series of experiment to study the effect of deposition time on the morphology of the NiCoFe composite obtained. Figure S1 shows the SEM images of the NiCoFe composites deposited on NF at different deposition time. At 50 seconds, a thin layer of nanostructured composites is formed, which grows larger with longer deposition time (150 seconds, Figure S1b), and finally forms a mesoporous structure with highly curved, rippled and interconnected nanoflakes (300 seconds, Figure S1c). Further prolonged deposition time induces no significant morphological change to the existing NiCoFe composites. Rather, extra nanoflakes begin to grow on the top of the existing NiCoFe porous layer, covering the nanopores (450 seconds, Figure S1d). With the further increase of deposition time, more and more pores will be blocked leading to decreased electrocatalytic performances. Therefore, the optimum deposition time in this study is determined to be 300 seconds. The elemental distributions of the three metal components in the NiCoFe composite are determined by Time-of-Flight secondary ion mass spectrometry (TOF-SIMS). Indexing in respective blue, green, and red, Ni, Co, and Fe are all found to distribute homogeneously in the NiCoFe composite (-Figure S2). Furthermore, from the ternary intensity histogram derived from Figure S2, it can be concluded that

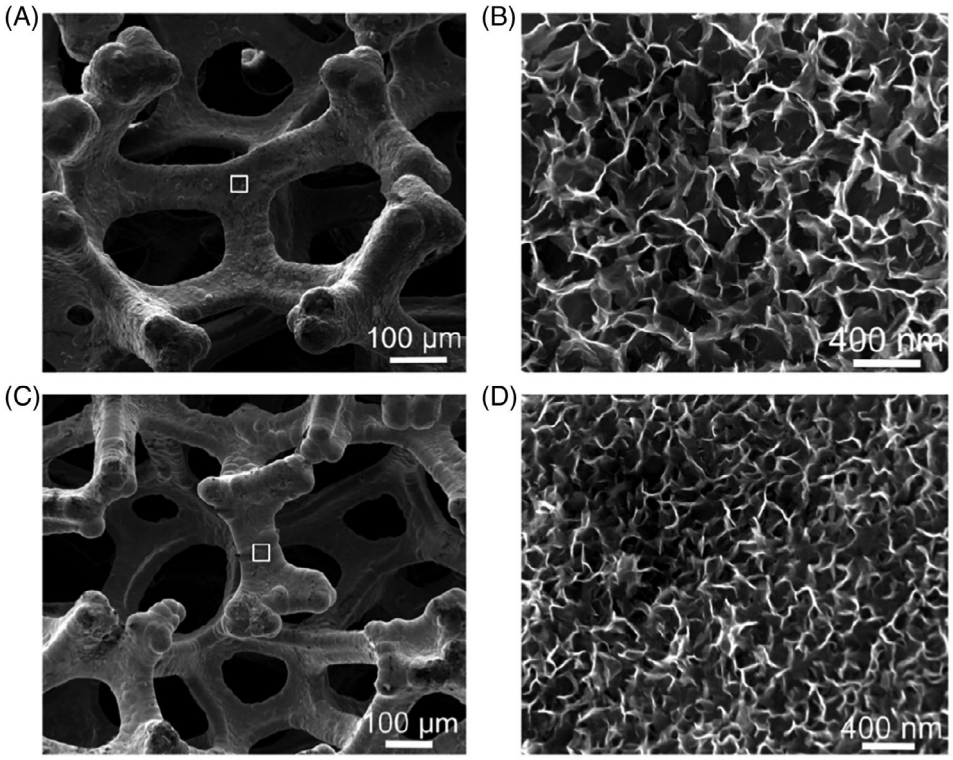

FIGURE 1 Scanning electron microscopy (SEM) images of the electrodes obtained. (A) NiCo/NF and (C) NiCoFe/NF. (B) and (D) are SEM images of the square marked in (A) and (C) under high magnifications, respectively

the Ni and Co contents in the NiCoFe composite are close to identical, but higher than the Fe content (Figure S3).

The chemical compositions of the NiCoFe/NF composite are analyzed by X-ray photoelectron spectroscopy (XPS). Figure S4 displays the XPS survey spectra of the NiCoFe/NF electrode. Only O, Ni, Fe, and Co elements can be detected in the XPS spectrum, confirming high purity electrodes can be obtained via the indirect electrodeposition technique. Figure 2 represents the high resolution Co 2p, Ni 2p, and Fe 2p XPS spectra of the NiCoFe/NF composite. The XPS results of NiCo/NF are also adopted for comparison. The two composites exhibit almost identical Co 2p and Ni 2p peaks (Figure 2). The Co 2p peaks can be fitted into two spin orbits, which belong to the Co $2p_{3/2}$ at 781.7 eV and Co $2p_{1/2}$ at 797.2 eV, respectively. Besides that, the energy separation between these two peaks is 15.5 eV, which is in good agreement with the data obtained for $Co(OH)_2$.[41,42] In the case of Ni 2p, two major peaks are detected at 857.2 and 874.8 eV, which belong to the spin orbit of Ni $2p_{3/2}$ and Ni $2p_{1/2}$, respectively. These two peaks have an energy separation of 17.6 eV, and are accompanied by two shake-up satellites, which are characteristic for the formation of $Ni(OH)_2$.[43,44] The distinction between the XPS spectra of NiCoFe/NF and NiCo/NF is observed in the Fe 2p spectrum, where NiCo/NF shows a broad and insidious peak, indicating the absence of Fe element in this composite. By contrast, in the NiCoFe/NF composite, the Fe 2p peak can be fitted into the Fe $2p_{3/2}$ and Fe $2p_{1/2}$ spin orbit at 712 and 725 eV, respectively, with a minor shake-up satellite in-between.[25] These data indicate that Fe is successfully incorporated into the NiCoFe composite, and presents mainly in the Fe^{3+} oxidation state.[45] Additionally, the O 1 second XPS spectrum of the NiCoFe/NF only exhibits one strong peak at 532.3 eV (Figure S5), corresponding to the bound hydroxide groups.[46] These collective data suggest that ternary NiCoFe hydroxide composite is formed on the NF substrate. Moreover, the atomic ratio of Ni, Co, and Fe in the composite is determined to be ~1:1:0.3 by performing the XPS characterization with NiCoFe composites deposited on platinum plate to bypass the strong signal interference arisen from the NF substrate. This data correlates well with the results obtained from TOF-SIMS (Figure S3).

The chemical compositions of the composite electrodes are also characterized by Raman spectroscopy (Figure S6). NF alone does not exhibit any significant peaks within the range tested. After the deposition of NiCo, two new peaks are observed at 453 and 534 cm^{-1}, which are ascribed to the symmetric Ni—OH stretching and the vibration of the Ni—O stretching.[47] Besides, the vibrational mode of $Co(OH)_2$ is also detected at 683 cm^{-1},[48] confirming successful preparation of the NiCo composites on NF. For the NiCoFe/NF composite, two additional peaks are observed at ~210 and 327 cm^{-1}, which are typical vibration peaks of $Fe(OH)_3$ and Fe—O,[47] also indicating the successful preparation of NiCoFe/NF. Figure S7 represents the XRD patterns of NiCoFe/NF and NiCo/NF. The bare NF is also included as a comparison. For all the samples tested herein, only three diffraction peaks at 44.5°, 51.8°, and 76.4° are detected, which are attributed to the nickel (111), (200), and (220) diffraction peaks from the NF.[49] No characteristic diffraction peaks belonging to the hydroxides of Ni, Co, and Fe, or their composites, are detected, suggesting that the as-deposited NiCoFe and NiCo composites on NF are both amorphous in nature. Figure S8 displays the transmission electron microscopy (TEM) images of NiCoFe composite carefully scratched off from the NF substrate. The NiCoFe composite exhibits a highly rippled sheet structure, without the observation of typical lattice fringes for Ni, Fe, and Co (Figure S8b), further confirming the as-prepared composite is amorphous.

2.2 | Electrochemical performances of NiCoFe/NF for OER

The electrocatalytic performances of the NiCoFe/NF electrode are firstly evaluated for OER in 1 M KOH using a standard three-electrode cell, employing NiCoFe/NF as the working electrode, a Ag/AgCl (sat. KCl) as the reference electrode and a Pt wire as the counter electrode. All

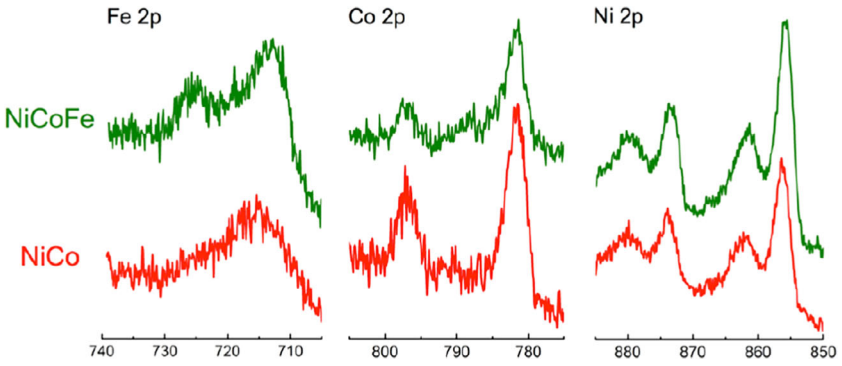

FIGURE 2 X-ray photoelectron spectroscopy (XPS) spectra in iron, cobalt, and nickel 2p regions. Green represents the NiCoFe/NF electrode, and red stands for the NiCo/NF electrode

potentials measured in this study are calibrated to the reversible hydrogen electrode (RHE, see details in Methods) for the comparison purpose. Before recording the polarization curves, the NiCoFe/NF electrode is continuously scanned in KOH solutions until a stable cyclic voltammogram (CV) is achieved. Figure S9 displays 20 consecutive CVs obtained with a freshly prepared NiCoFe/NF electrode in 1 M KOH in the potential range for OER. It can be seen from Figure S9 that during the first several cycles, an increase of OER catalytic activity is observed, which then stabilizes after about 10 cycles. No significant change in OER activity is observed even after 20 cycles. As shown in Figure. 3A, the onset of OER is observed at 1.45 V, corresponding to an overpotential of merely 220 mV. The oxidation peak prior to OER is ascribed to the oxidative formation of catalytic active NiOOH and CoOOH sites.[50,51] The *i*R corrected curve displays an identical onset potential but much higher current densities at the same applied voltages. At 1.53 V (η = 300 mV), a current density of 100 mA cm^{-2} can be achieved. The high OER activity of NiCoFe/NF is ascribed to the ternary NiCoFe hydroxide deposited on NF, since pure NF exhibits negligible OER catalytic activity at even higher potentials, for example, 1.55 V (Figure 3A). Figure 3B represents the Tafel plot of NiCoFe/NF obtained at a slow scan rate of 0.1 mV s^{-1}, to minimize the influence of the Ni^{2+} and Co^{2+} oxidation processes.[25] Useful information including the onset of linearity (E_{cat}) and Tafel slope, are obtained from the Tafel plot. The E_{cat} is the potential where the linear dependence of potential on current density starts, representing the initiation of water oxidation. After the linear part, the current density is limited by the electron transfer kinetic and mass transport. The E_{cat} derived from the Tafel plot is 1.45 V. According to the Tafel plot, the potential required to obtain a current density of 10 mA cm^{-2} is 1.47 V, which corresponds to an overpotential of only 240 mV. The Tafel plot shows a slope of 50 mV dec^{-1} and remains good linearity even under high current density of 100 mA cm^{-2}, indicating the good electrical contact between the deposited NiCoFe composites and the NF substrates.

The OER catalytic activity of NiCoFe/NF is also compared with some advanced OER electrocatalysts reported previously and the results are summarized in Table S1 and Table S2. NiCoFe/NF requires the lowest overpotential (240 mV) among all the catalysts listed in Table S1 to deliver a current density of 10 mA cm^{-2}, a value relative to solar fuel synthesis because this current density roughly matches the spectrum for a 10% efficient solar-to-hydrogen fuel device.[52,53] Furthermore, the superior OER catalytic activity of NiCoFe/NF is verified by using electrochemical active surface area (ECAS) according to the methods established previously,[54] and

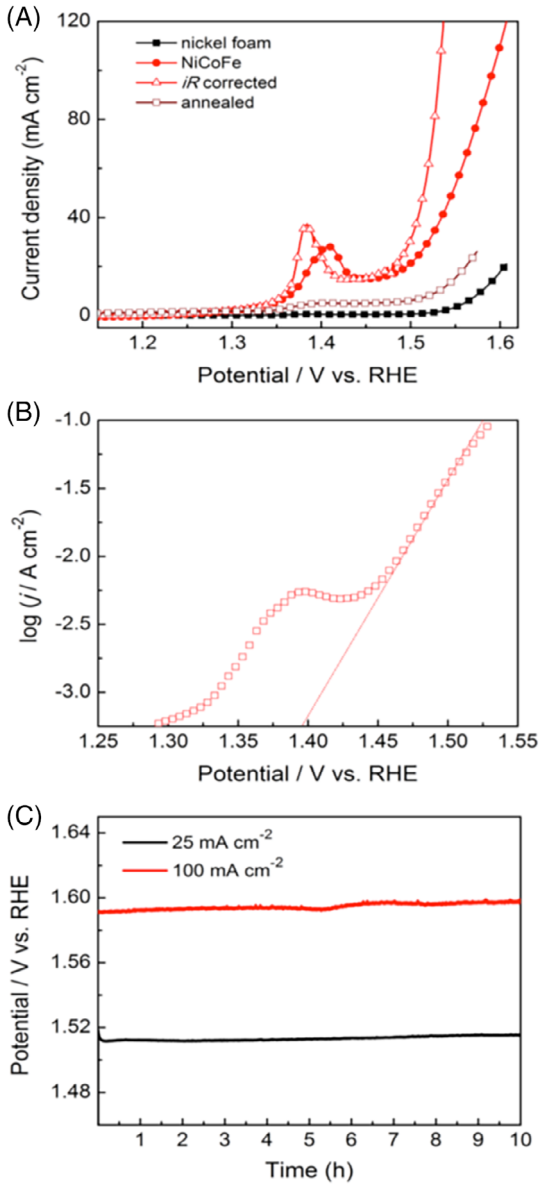

FIGURE 3 Oxygen evolution performances of the NiCoFe/NF electrode. (A) oxygen evolution reaction (OER) polarization curves of nickel foam, NiCoFe/NF and NiCoFe/NF that has been annealed at 300°C for 2 hours in 1 M KOH solution obtained at 5 mV s^{-1}. (B) Tafel plot obtained for NiCoFe/NF composite in 1 M KOH at 0.1 mV s^{-1} with 95% *i*R compensation. (C) Chronoampermetric measurements of the NiCoFe/NF composite in 1 M KOH obtained at constant current densities of 25 and 100 mA cm^{-2}, respectively

the results are summarized in Table S2. At the same overpotential of 350 mV, NiCoFe/NF exhibits the highest current density using either geometric surface area (GSA) or ECAS, which is more than one order of magnitude higher than the benchmark IrO_x catalyst, and is also superior to other non-precious metal-based OER catalysts. Moreover, we have also compared the OER catalytic activity of the as-prepared NiCoFe/NF electrode with the state-of-the-art NiCo and NiFe catalysts, and the results

are summarized in Table S3. It can be seen that the NiCoFe/NF electrode shows significantly higher current density, normalized either by surface area or mass loading, than the reported NiCo and NiFe catalysts at the overpotential of 300 mV. The collective data indicate that the NiCoFe/NF is one of the most active OER catalysts in alkaline media reported so far.

The long-term stability of NiCoFe/NF under OER is evaluated in prolonged bulk electrolysis of water. Figure 3C shows the chronopotentiometric curves obtained with NiCoFe/NF at current densities of 25 and 100 mA cm^{-2}, respectively. A potential of 1.51 V is required to deliver a current density of 25 mA cm^{-2}, which remains constant during the 10 hours of water electrolysis. At a much higher current density of 100 mA cm^{-2}, the potential starts with ~1.59 V, and also remains stable (<5 mV increment) during the 10 hours electrolysis. The physical stability of NiCoFe/NF in OER is further confirmed by SEM (Figure S10). The morphology of the deposited NiCoFe composite remains essentially unchanged. The above data show that the NiCoFe/NF is a stable catalyst for continuous OER.

Figure 3A also represents the OER polarization curves obtained with NiCoFe/NF before and after 2 hours annealing at 300°C. The heating treatment has severely impaired the OER catalytic activity of the NiCoFe/NF, showing ~50 mV positive shift of onset potential and significantly lowered current density at a given potential, for example, at 1.53 V. This observation suggests the advantages of utilizing amorphous structures over their crystalline compartments in electrochemical applications, which is in accordance to the results obtained in other studies.[12,43,55]

2.3 | Electrochemical performances of NiCoFe/NF for HER

HER is the counter reaction of OER in water electrolysis. Even though HER requires relatively low overpotential to obtain a decent current density compared to OER, it however requires precious metal-based catalysts such as Pt.[56,57] For Earth-abundant materials, the overpotential of HER is usually significantly higher. In this study, the NiCoFe/NF electrode is also investigated as the working electrode for HER. Figure 4A represents the HER polarization curves obtained with the NiCoFe/NF electrode. The *i*R corrected curve shows an HER onset potential of −0.05 V (inset in Figure 4A), corresponding to an overpotential of merely 50 mV. Current densities of 10 and 100 mA cm^{-2} are obtained at −0.083 and − 0.21 V, respectively, from the *i*R corrected polarization curve. Table S4 lists the HER catalytic activity of NiCoFe/NF compared with state-of-the-art HER catalysts. Even though our catalyst loading is significantly lower, the HER activity of the NiCoFe/NF electrode, (eg, the overpotentials required to deliver current densities at 10 and 100 mA cm^{-2}) is among the highest.

The high HER activity is attributed to the NiCoFe composite deposited on NF, as the pure NF shows much lower HER catalytic activities compared with the NiCoFe/NF (Figure 4A). The Tafel slope of NiCoFe/NF in HER is 80 mV dec^{-1} (Figure 4B), which is similar to other nonprecious metal-based catalysts such as CuMoS, NiMo, and NiCo.[58-60] The stability of NiCoFe/NF in HER

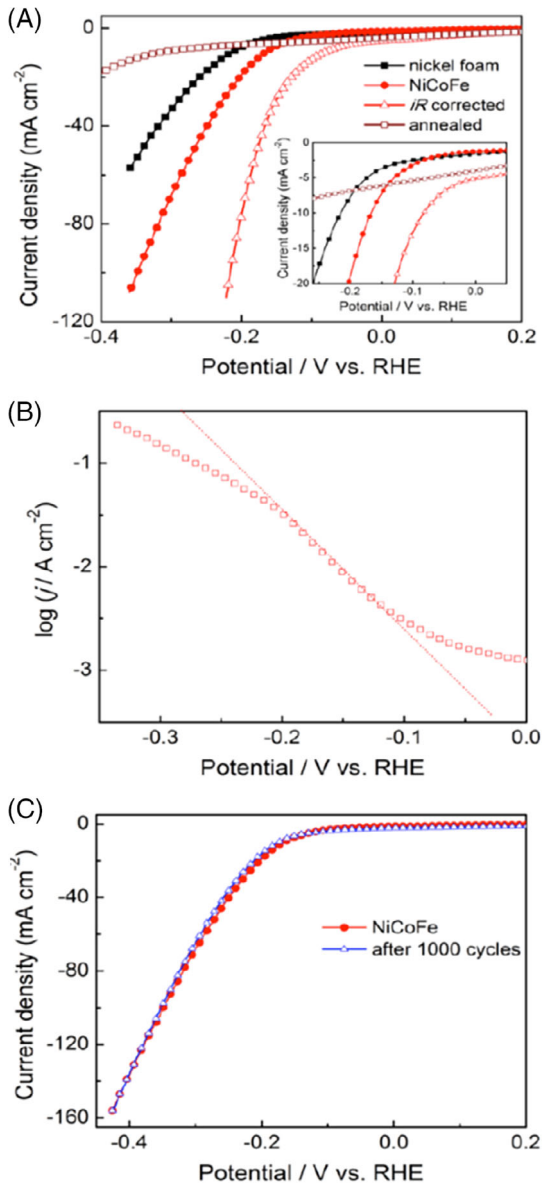

FIGURE 4 Hydrogen evolution performances of the NiCoFe/NF electrode. (A) hydrogen evolution reaction (HER) polarization curves of nickel foam. NiCoFe/NF and NiCoFe/NF that has been annealed at 300°C for 2 hours in 1 M KOH solution at 5 mV s^{-1}. (B) Tafel plot of the NiCoFe/NF composite in 1 M KOH at 0.1 mV s^{-1} with 95% *i*R compensation. (C) HER polarization curves of NiCoFe/NF obtained before and after 1000 potential scans from 0.45 V to −0.55 V in 1 M KOH solution at 5 mV s^{-1}

is prominent, with identical polarization curves obtained even after 1000 cycles of voltage scan in the range of −0.45 to 0.55 V (Figure 4C). Figure 4A also represents the effect of annealing on the HER performance of NiCoFe/NF. Similar to OER, the HER catalytic activity of NiCoFe/NF is also dramatically decreased after the annealing treatment, further indicating the benefits of utilizing amorphous NiCoFe/NF in water electrolysis.

2.4 | The effect of Ni, Co, and Fe content on NiCoFe/NF for OER and HER

Initially, the ratio between Ni and Co has been systematically varied so as to investigate their roles in affecting the catalytic activities. As shown in Figure S11a and S11b, three NiCo composites were deposited on NF from electrolytes containing Ni^{2+} and Co^{2+} in ratios of 1:1, 2:1, and 1:2, and their catalytic activity toward both OER and HER are evaluated. As can be seen from Figure S11a and S11b, the effects of Ni/Co ratio on OER and HER performance are not significant. Therefore, we fixed the Ni/Co ratio at 1:1 and prepared a series of ternary NiCoFe composites with different Fe content by varying the molar ratio of Ni^{2+}, Co^{2+}, and Fe^{3+} in the electrolytes during electrodeposition, and their structures and corresponding electrochemical performances compared. At a low Fe content, the trimetallic composite exhibits the nanoflake structure (Figure 1B,D and S12a). With increasing Fe content, the NiCoFe composite gradually transforms to a nanosheet structures (Figure S12b-c), forming smaller pore sizes.

The electrochemical performances of these NiCoFe/NF composites are evaluated with CVs as shown in Figure 5. The bimetallic NiCo/NF composite exhibits reversible redox process regarding the formation of NiOOH and CoOOH with large areal current densities, indicating NiCo/NF as a promising electrode material for pseudocapacitors.[61] Incorporation of Fe into NiCo composites on one hand significantly suppresses the redox processes, resulting in smaller areal current densities. On the other hand, the OER catalytic activity has been enhanced dramatically in the presence of Fe. All composites containing Fe exhibit superior OER catalytic performance to the NiCo/NF, as suggested by negatively shifted onset potentials and higher current densities obtained for a given potential (Figure 5). NiCoFe/NF prepared from electrolytes containing equal molar of Ni^{2+}, Co^{2+}, and Fe^{3+} (1.67 mM) has the highest OER catalytic activity, while a further increase in Fe content leads to receded OER performances. XPS spectra obtained with NiCoFe/NF before and after prolonged bulk OER tests are identical (Figure S4 and Figure S13), suggesting no contamination or variation of the composition of the NiCoFe catalyst during the electrolysis.

The effects of Fe in the composites on OER can be attributed to several possible factors. (a) It has been established that the incorporation of Fe can enhance the electrical conductivity of MOOH (M = Ni and Co), therefore facilitate the electron transport during electrocatalytic reactions, such as OER and HER.[23,62] (b) A more defective structure of catalysts might appear upon the incorporation of Fe into the NiCo oxyhydroxide, thusly results in a faster HER kinetics by accelerating the water dissociation process (Volmer step).[33] (c) Fe may exert a partial-charge-transfer activation effect on Ni and/or Co, similar to that observed for Au electrode surfaces.[19] Adding Fe stabilizes Ni and/or Co in a higher oxidation level with more oxidizing power and therefore faster OER kinetics. However, the presence of excessive Fe can sacrifice the catalytic active Co and Ni sites, lowering the OER performance. The effect of Fe on HER is not as significant as that on OER. Figure 5 shows that all samples exhibit high catalytic activity in HER, with little change upon the variation of Fe content. Thus, the NiCoFe/NF prepared from electrolytes containing equal molar of Ni^{2+}, Co^{2+}, and Fe^{3+} is optimal for both OER and HER in water electrolysis.

2.5 | Overall water electrolysis using two NiCoFe/NF electrodes

The NiCoFe/NF electrode is further employed in a two-electrode water electrolysis cell for overall water electrolysis and the energy efficiency during water electrolysis is determined (Figure S14). Figure S15 displays the

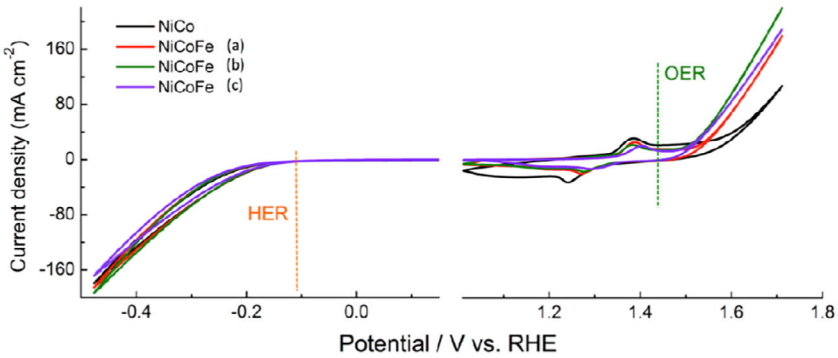

FIGURE 5 Effect of iron content on the oxygen evolution reaction (OER) and hydrogen evolution reaction (HER) performances. cyclic voltammograms (CVs) of NiCo bimetallic and NiCoFe trimetallic hydroxide composites with different Fe content deposited on nickel foam obtained in 1 M KOH solution at 5 mV s^{-1}. NiCoFe composites were prepared from electrolytes containing Ni^{2+}, Co^{2+}, and Fe^{3+} ions at ratios of (A) 1:1:0.5, (B) 1:1:1, and (C) 1:1:1.5, respectively

chronoamperometric curve obtained with the NiCoFe/NF anode and cathode in 1 M KOH. The overall water electrolysis reaction can be initiated at applied voltages around 1.50 V, the typical output an ordinary AAA battery, with the observation of continuous and stable evolution of bubbles on both electrodes. At an applied cell potential of 1.53 V, a stabilized current density around 3 mA cm^{-2} is achieved corresponding to a whole cell overpotential of 300 mV and an energy efficiency of 80.4% (see details in Methods). At higher current densities such as 10 and 25 mA cm^{-2} (Figure S16), the energy efficiencies drop to 68.0% and 64.1%, respectively, mainly attributed to the *i*R drop arisen from the electrolytes.[63]

Compared with recently reported bifunctional catalysts in two-electrode overall water splitting, the NiCoFe/NF electrode requires higher voltage to obtain relatively high current densities, such as 10 mA cm^{-2} (Table S5). However, this difference can be ascribed to the relatively low loading of NiCoFe catalysts on NF. To achieve reasonable performances in two-electrode water splitting, a common strategy is to load larger amounts of catalyst onto current collectors so as to overcome the sluggish reaction kinetics as well as slow mass transportations that normally encountered with two-electrode water electrolysis. As shown in Table S5, the catalyst loading is normally >2 mg cm^{-2}. However, in our case, the loading of NiCoFe is only about 0.11 mg cm^{-2}, as determined by electrochemical quartz crystal microbalance using the method described somewhere else.[38] Therefore, if all current densities obtained are normalized by the mass of catalysts (j_{mass}), the NiCoFe/NF electrode clearly exhibits higher intrinsic catalytic activity as reflected by larger j_{mass} even at a lower applied voltage (Table S5). Figure 6A exhibits the oxygen and hydrogen concentration profiles during the course of two-electrode water electrolysis at a constant current density of 8 mA cm^{-2} using NiCoFe/NF as both the anode and the cathode. As predicted, the amount of hydrogen and oxygen detected by gas chromatography show a volume ratio of 2:1, and Faraday efficiencies obtained are always close to unity for both OER and HER, suggesting oxygen and hydrogen are the only products and overall water splitting is achieved.

The stability of NiCoFe/NF electrodes is further tested under continuous and intermittent operations. Figure 6B represents the chronoamperometric curves obtained in a two-electrode water electrolysis system employing NiCoFe/NF as both the anode and the cathode in 1 M KOH. A constant potential of 1.53 V was first applied between the two electrodes for 1 hour, then the power was shut down for half an hour to mimic a power interruption. The corresponding current density was recorded to verify the electrode stability. Figure 6B shows that upon switching on the power the current density of ~3 mA cm^{-2} is obtained and remain stable during 1 hour bulk water electrolysis. When the power is switched on again after 30 minutes shutdown, the current density resumes ~3 mA cm^{-2}, after the initial spike of

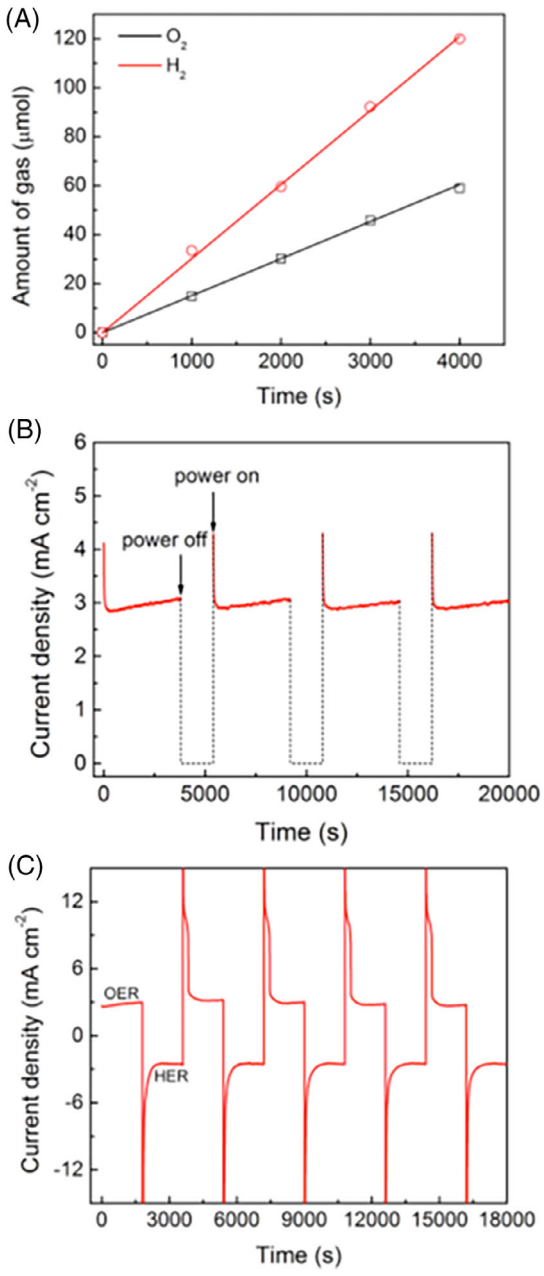

FIGURE 6 Water electrolysis performance obtained in the two-electrode system employing NiCoFe/NF as both the anode and cathode in 1 M KOH. (A) Amount ratio and Faraday efficiency of oxygen and hydrogen detected by gas chromatography in the two electrode system at a current density of 8 mA cm^{-2}. (B) Chronoamperometric curves obtained with the NiCoFe/NF anode and cathode during power interruptions. The applied potential is 1.53 V, and the periods for continuous electrolysis and power shutdowns are 1 and 0.5 hour, respectively. (C) Chronoamperometric curves obtained with the NiCoFe/NF anode and cathode under an applied potential of 1.53 V. The polarity of electrode is reversed every 30 minutes

capacitive current, and remains unchanged in each cycle of power interruption. In contrast, in a two electrode electrolysis cell using the benchmark Pt/C and Ir/C catalysts as the cathode and anode respectively, the current density decreases by 40% after three showdowns (Figure S17a). The results demonstrate that NiCoFe/NF has excellent time stability and durability under condition of intermittent electrolysis.

We further studied the robustness of the NiCoFe/NF electrode for intermittent electrolysis by electrochemical oxidation/reduction treatments, which give the more severe effect on the electrocatalytic activity. In this experiment, the polarity of two NiCoFe/NF electrodes in the cell is reversed every half an hour, and each NiCoFe/NF electrode is used for HER and OER alternately. Under such conditions, taking HER for example, the NiCoFe/NF electrode is subjected to anodic oxidation for half an hour before HER is resumed. As can be seen from Figure 6C, when the NiCoFe/NF is used as the anode at 1.53 V, the OER current density stabilizes at 3 mA cm^{-2}. When electrode polarity is changed to cathode, the current changes swiftly to −3 mA cm^{-2} for HER. No decay in current density is observed after the electrode polarity is reversed for nine cycles, In comparison, as shown in Figure S17b, the benchmark Ir/C and Pt/C catalysts exhibit poor stability upon polarity change, as reflected by gradual decrease in current density for both OER and HER after each cycle. The above results suggest the as-prepared NiCoFe/NF is fully reversible and interexchangeable between OER and HER during water electrolysis.

It is noteworthy that when the NiCoFe/NF electrode polarity is switched back to anode, a small current stair is observed before the OER current stabilizes again at 3 mA cm^{-2}. This is ascribed to the oxidation of absorbed hydrogen generated during HER at the NiCoFe/NF electrode, as when the absorbed hydrogen gas from HER is removed by exposing the electrode into air, the current stair is no longer detected in the subsequent anodic current (Figure S18). This could be attributed to the hydrogen storage capacity of the Ni and/or Co-based alloys, which is usually beneficial to the corrosion resistance properties of the electrode during shutdowns.[15,64] Intriguingly, the NiCoFe/NF catalysts exhibit distinctly different color when used for OER (black) and HER (silver grey), as shown in Figure S14, attributed to transformation of the transition metal components in the electrode to different oxidation states, for example, from transparent Ni^{2+} to black Ni^{3+}. It is observed that in Figure 6C that reversing the electrode polarity and current direction is accompanied with the change of the electrode color and the process is reproducible for each cycle. Notably, the reproducible changes of the electrode color upon the frequent switches of electrode polarity might be ascribed to the reversible transformation of two catalytic forms (for OER and HER, respectively), and that endows the NiCoFe/NF electrode a prolonged stability as well as robust reversibility between OER and HER under the different operation bias.[33]

3 | CONCLUSION

Free standing ternary NiCoFe hydroxide composite catalysts have been obtained via a facile electrodeposition method onto NF substrates, and applied as cost-effective, efficient bifunctional electrodes for reversible water splitting under continuous and intermittent conditions. The electrodes exhibit distinctive electrochemical performances upon the variations of Fe content, showing the highest catalytic activity when deposited from electrolytes comprised of equal molar of Ni^{2+}, Co^{2+}, and Fe^{3+} (NiCoFe/NF). The results in this study suggest that the Fe content can be used as an indicator for designing trimetallic NiCoFe hydroxide composite catalysts toward specific applications. The high catalytic performances of the bifunctional NiCoFe/NF electrode for both OER and HER makes it a potential candidate to substitute all precious metal components such as Ru and Ir-based anode and Pt-based cathode materials in a water electrolyzer. Thus, a highly efficient and robust water electrolyzer employing two inexpensive NiCoFe/NF electrodes can be used for continuous and intermittent water electrolysis for industrial-scale hydrogen production and renewable energy storage.

4 | EXPERIMENTAL SECTION

Preparation of NiCoFe/NF: The nickel foam (thickness: 1.6 mm, bulk density: 0.45 g cm^{-3}, Goodfellow) was first sonicated in 5 M HCl solution for 20 minutes to remove the NiOx layer on the surface, rinsed subsequently with water and ethanol, and then dried in air. The electrodeposition was carried out in a standard three-electrode electrochemical cell. The NF was used as the working electrode, together with a parallel positioned platinum plate auxiliary electrode and a Ag/AgCl (3 M KCl) reference electrode. To obtain trimetallic composites, Milliq water (~18.1 MΩ) dissolved with x mM $Ni(NO_3)_2{\cdot}6H_2O$, x mM $Co(NO_3)_3{\cdot}6H_2O$ and y mM $Fe(NO_3)_3{\cdot}9H_2O$ ($2x + y = 5$) was used as the electrolyte ($y = 0$ for NiCo bimetallic composite). The electrodeposition was conducted with a CHI 760 Electrochemical Workstation (CH Instrument) at −1.0 V (vs Ag/AgCl) for 300 seconds under ambient conditions and the electrodeposition curve is shown in Figure S19. After deposition, the NF

was carefully withdrawn from the electrolyte, rinsed thoroughly with water and ethanol, and left dry in air. NiCoFe was also electrodeposited on Pt plate according to the same procedure.

Physical characterization: XPS was performed on a Thermo ESCALAB250i X-ray Photoelectron Spectrometer. SEM was carried out using a FEI Nova NanoSEM 230 with a 10 kV accelerating voltage. TEM was performed using a Philips CM 200 microscope. Raman spectroscopy was performed using a laser micro-Raman spectrometer (Renishaw) employing a laser with an incident wavelength of 514.5 nm. XRD was performed on a PANalytical X'Pert instrument. TOF-SIMS was performed on a TOF.SIMS 5 instrument.

Electrochemical characterization: All electrochemical measurements were carried out with a CHI 760 electrochemical workstation in 1 M KOH solution (pH = 14). The NiCoFe/NF electrodeposited from electrolyte containing equal molar of Ni^{2+}, Co^{2+}, and Fe^{3+} was used as the working electrode without further treatments. The electrochemical characterizations were conducted in a standard three-electrode electrochemical cell employing a Pt wire (or a graphite rod for HER tests) and a Ag/AgCl (sat. KCl) as the counter and the reference electrode, respectively. All potentials measured were calibrated to RHE using the following equation: $E_{RHE} = E_{Ag/AgCl} + 0.197\ V + 0.059\ pH$. All measurements were carried out at a scan rate of 5 mV s^{-1}. Tafel plots were derived from OER and HER polarization curves obtained at a scan rate of 0.1 mV s^{-1} with 95% corrected *i*R drop using NiCoFe/NF as the working electrode. Chronopotentiometric and chronoampermetric measurements were obtained under the same experimental setup without compensating iR drop. The *i*R drop was determined automatically using the potentiostat.

CONFLICT OF INTEREST

C.Z. and X.L. filed an International Patent Application (no. PCT/AU2015/000478) on the basis of the work reported in this paper.

ACKNOWLEDGEMENTS

All the physical characterizations were carried out in Mark Wainwright Analytical Centre (MWAC) at the University of New South Wales (UNSW). We thank Dr Bin Gong from MWAC for his assistance in XPS and TOF-SIMS measurements. The study was financed by an ARC Discovery Grant (DP160103107).

ORCID

Qingran Zhang https://orcid.org/0000-0002-9939-8383
Chuan Zhao https://orcid.org/0000-0001-7007-5946

REFERENCES

1. She ZW, Kibsgaard J, Dickens CF, Chorkendorff I, Nørskov JK, Jaramillo TF. Combining theory and experiment in electrocatalysis: insights into materials design. *Science*. 2017; 355:eaad4998.
2. Liu B, Wang Y, Peng H, et al. Iron vacancies induced bifunctionality in ultrathin feroxyhyte nanosheets for overall water splitting. *Adv Mater*. 2018;30:1803144.
3. Zhao S, Wang Y, Dong J, et al. Ultrathin metal–organic framework nanosheets for electrocatalytic oxygen evolution. *Nat Energy*. 2016;1:16184.
4. Lee Y, Suntivich J, May KJ, Perry EE, Shao-Horn Y. Synthesis and activities of rutile IrO_2 and RuO_2 nanoparticles for oxygen evolution in acid and alkaline solutions. *J Phys Chem Lett*. 2012;3:399-404.
5. Blakemore JD, Schley ND, Olack GW, Incarvito CD, Brudvig GW, Crabtree RH. Anodic deposition of a robust iridium-based water-oxidation catalyst from organometallic precursors. *Chem Sci*. 2011; 2:94-98.
6. Reier T, Oezaslan M, Strasser P. Electrocatalytic oxygen evolution reaction (OER) on Ru, Ir, and Pt catalysts: a comparative study of nanoparticles and bulk materials. *ACS Catal*. 2012;2: 1765-1772.
7. Sheng W, Gasteiger HA, Shao-Horn Y. Hydrogen oxidation and evolution reaction kinetics on platinum: acid vs alkaline electrolytes. *J Electrochem Soc*. 2010;157:B1529-B1536.
8. Yin H, Zhao S, Zhao K, et al. Ultrathin platinum nanowires grown on single-layered nickel hydroxide with high hydrogen evolution activity. *Nat Commun*. 2015;6:6430.
9. Yan Y, Xia BY, Zhao B, Wang X. A review on noble-metal-free bifunctional heterogeneous catalysts for overall electrochemical water splitting. *J Mater Chem A*. 2016;4:17587-17603.
10. Lu X, Zhao C. Highly efficient and robust oxygen evolution catalysts achieved by anchoring nanocrystalline cobalt oxides onto mildly oxidized multiwalled carbon nanotubes. *J Mater Chem A*. 2013;1:12053-12059.
11. Wang J, Cui W, Liu Q, Xing Z, Asiri AM, Sun X. Recent progress in cobalt-based heterogeneous catalysts for electrochemical water splitting. *Adv Mater*. 2016;28:215-230.
12. Zhang B, Zheng X, Voznyy O, et al. Homogeneously dispersed multimetal oxygen-evolving catalysts. *Science*. 2016; 352:333-337.
13. Song F, Hu X. Exfoliation of layered double hydroxides for enhanced oxygen evolution catalysis. *Nat Commun*. 2014;5: 4477.
14. Janjua MBI, Roy RLLE. Electrocatalyst performance in industrial water electrolysers. *Int J Hydrogen Energy*. 1985;10:11-19.
15. Lei Z, Bai J, Li Y, Wang Z, Zhao C. Fabrication of nanoporous nickel-iron hydroxylphosphate composite as bifunctional and reversible catalyst for highly efficient intermittent water splitting. *ACS Appl Mater Interfaces*. 2017;9:35837-35846.
16. Zhang P, Li L, Nordlund D, et al. Dendritic core-shell nickel-iron-copper metal/metal oxide electrode for efficient electrocatalytic water oxidation. *Nat Commun*. 2018;9:381.
17. Enman L, Burke Stevens M, Dahan M, Nellist M, Caspary Toroker M, Boettcher S. Operando X-ray absorption spectroscopy shows Fe oxidation is concurrent with oxygen evolution in cobalt-iron (oxy)hydroxide electrocatalysts. *Angew Chem Int Ed*. 2018;57:12840-12844.

18. Liu J, Ji Y, Nai J, et al. Ultrathin amorphous cobalt-vanadium hydr(oxy)oxide catalysts for oxygen evolution reaction. *Energ Environ Sci*. 2018;11:1736-1741.
19. Trotochaud L, Young SL, Ranney JK, Boettcher SW. Nickel-iron oxyhydroxide oxygen-evolution electrocatalysts: the role of intentional and incidental iron incorporation. *J Am Chem Soc*. 2014;136:6744-6753.
20. Burke MS, Kast MG, Trotochaud L, Smith AM, Boettcher SW. Cobalt-iron (oxy)hydroxide oxygen evolution electrocatalysts: the role of structure and composition on activity, stability, and mechanism. *J Am Chem Soc*. 2015;137:3638-3648.
21. Kuang Y, Kenney MJ, Meng Y, et al. Solar-driven, highly sustained splitting of seawater into hydrogen and oxygen fuels. *Proc Natl Acad Sci*. 2019;116:6624-6629.
22. Li N, Bediako DK, Hadt RG, et al. Influence of iron doping on tetravalent nickel content in catalytic oxygen evolving films. *Proc Natl Acad Sci*. 2017;114:1486-1491.
23. Xu YF, Gao MR, Zheng YR, Jiang J, Yu SH. Nickel/nickel (II) oxide nanoparticles anchored onto cobalt(IV) diselenide nanobelts for the electrochemical production of hydrogen. *Angew Chem Int Ed*. 2013;52:8546-8550.
24. Schäfer H, Kuepper K, Koppe J, et al. Intercalation of Li^+ into a co-containing steel-ceramic composite: substantial oxygen evolution at almost zero overpotential. *ACS Catal*. 2018;8:10914-10925.
25. Jin H, Wang J, Su D, Wei Z, Pang Z, Wang Y. In situ cobalt−cobalt oxide/N-doped carbon hybrids as superior bifunctional electrocatalysts for hydrogen and oxygen evolution. *J Am Chem Soc*. 2015;137:2688-2694.
26. Jiang N, You B, Sheng M, Sun Y. Electrodeposited cobalt-phosphorous-derived films as competent bifunctional catalysts for overall water splitting. *Angew Chem Int Ed*. 2015;54:6251-6254.
27. Cobo S, Heidkamp J, Jacques P-A, et al. A Janus cobalt-based catalytic material for electro-splitting of water. *Nat Mater*. 2012;11:802-807.
28. Luo J, Im J-H, Mayer MT, et al. Water photolysis at 12.3% efficiency via perovskite photovoltaics and Earth-abundant catalysts. *Science*. 2014;345:1593-1596.
29. Schäfer H, Sadaf S, Walder L, et al. Stainless steel made to rust: a robust water-splitting catalyst with benchmark characteristics. *Energ Environ Sci*. 2015;8:2685-2697.
30. Yang Y, Yao H, Yu Z, et al. Hierarchical nanoassembly of $MoS_2/Co_9S_8/Ni_3S_2$/Ni as a highly efficient wide-pH range electrocatalyst for overall water splitting. *J Am Chem Soc*. 2019;141:10417-10430.
31. Zhang Q, Webster RF, Cheong S, Tilley RD, Lu X, Amal R. Ultrathin Fe-N-C nanosheets coordinated Fe-doped CoNi alloy nanoparticles for electrochemical water splitting. *Part Syst Charact*. 2019;36:1800252.
32. Rafailović LD, Gammer C, Rentenberger C, Trišović T, Kleber C, Peter Karnthaler H. Enhanced oxygen evolution and reduction reactions of porous ternary NiCoFe foam electrodes prepared by dynamic hydrogen template deposition. *Nano Energy*. 2013;2:523-529.
33. Zhang Q, Bedford NM, Pan J, Lu X, Amal R. A fully reversible water electrolyzer cell made up from FeCoNi (oxy)hydroxide atomic layers. *Adv Energy Mater*. 2019;9:1901312.
34. Ji J, Zhang LL, Ji H, et al. Nanoporous $Ni(OH)_2$ thin film on 3D ultrathin-graphite foam for asymmetric supercapacitor. *ACS Nano*. 2013;7:6237-6243.
35. Chaudhari NK, Jin H, Kim B, Lee K. Nanostructured materials on 3D nickel foam as electrocatalysts for water splitting. *Nanoscale*. 2017;9:12231-12247.
36. Zhou H, Yu F, Sun J, et al. Highly active catalyst derived from a 3D foam of $Fe(PO_3)_2/Ni_2P$ for extremely efficient water oxidation. *Proc Natl Acad Sci*. 2017;114:5607-5611.
37. Hao R, Fan Y, Howard MD, Vaughan JC, Zhang B. Imaging nanobubble nucleation and hydrogen spillover during electrocatalytic water splitting. *Proc Natl Acad Sci*. 2018;115:5878-5883.
38. Lu X, Zhao C. Electrodeposition of hierarchically structured three-dimensional nickel–iron electrodes for efficient oxygen evolution at high current densities. *Nat Commun*. 2015;6:6616.
39. Zhao DD, Bao SJ, Zhou WJ, Li HL. Preparation of hexagonal nanoporous nickel hydroxide film and its application for electrochemical capacitor. *Electrochem Commun*. 2007;9:869-874.
40. Zhao J, Li Z, Yuan X, et al. A high-energy density asymmetric supercapacitor based on Fe_2O_3 nanoneedle arrays and $NiCo_2O_4/Ni(OH)_2$ hybrid nanosheet arrays grown on SiC nanowire networks as free-standing advanced electrodes. *Adv Energy Mater*. 2018;8:1-14.
41. Pi Y, Shao Q, Wang P, et al. Trimetallic oxyhydroxide coralloids for efficient oxygen evolution electrocatalysis. *Angew Chem Int Ed*. 2017;56:4502-4506.
42. Li Z, Wang J, Niu L, et al. Rapid synthesis of graphene/cobalt hydroxide composite with enhanced electrochemical performance for supercapacitors. *J Power Sources*. 2014;245:224-231.
43. Li P, Duan X, Kuang Y, et al. Tuning electronic structure of NiFe layered double hydroxides with vanadium doping toward high efficient electrocatalytic water oxidation. *Adv Energy Mater*. 2018;8:1703341.
44. Yu X, Zhao J, Zheng LR, et al. Hydrogen evolution reaction in alkaline media: alpha- or beta-nickel hydroxide on the surface of platinum? *ACS Energy Lett*. 2018;3:237-244.
45. Ye SH, Shi ZX, Feng JX, Tong YX, Li GR. Activating CoOOH porous nanosheet arrays by partial iron substitution for efficient oxygen evolution reaction. *Angew Chem Int Ed*. 2018;57:2672-2676.
46. Gong L, Chng XYE, Du Y, Xi S, Yeo BS. Enhanced catalysis of the electrochemical oxygen evolution reaction by iron(III) ions adsorbed on amorphous cobalt oxide. *ACS Catal* 2018;8:807–814.
47. Oliver-Tolentino MA, Vázquez-Samperio J, Manzo-Robledo A, et al. An approach to understanding the electrocatalytic activity enhancement by superexchange interaction toward OER in alkaline media of Ni-Fe LDH. *J Phys Chem C*. 2014;118:22432-22438.
48. Long X, Xiao S, Wang Z, Zheng X, Yang S. Co intake mediated formation of ultrathin nanosheets of transition metal LDH-an advanced electrocatalyst for oxygen evolution reaction. *Chem Commun*. 2015;51:1120-1123.
49. Guo CX, Li CM. Room temperature-formed iron-doped nickel hydroxide on nickel foam as a 3D electrode for low polarized and high-current-density oxygen evolution. *Chem Commun*. 2018;54:3262-3265.
50. Yeo BS, Bell AT. Enhanced activity of gold-supported cobalt oxide for the electrochemical evolution of oxygen. *J Am Chem Soc*. 2011;133:5587-5593.
51. Louie MW, Bell AT. An investigation of thin-film Ni-Fe oxide catalysts for the electrochemical evolution of oxygen. *J Am Chem Soc*. 2013;135:12329-12337.

52. Tan CS, Kemp KW, Braun MR, et al. >10% solar-to-hydrogen efficiency unassisted water splitting on ALD-protected silicon heterojunction solar cells. *Sustain Energy Fuels*. 2019;3:1490-1500.
53. Kuhl KP, Cave ER, Abram DN, Jaramillo TF. New insights into the electrochemical reduction of carbon dioxide on metallic copper surfaces. *Energ Environ Sci*. 2012;5:7050-7059.
54. McCrory CCL, Jung S, Peters JC, Jaramillo TF. Benchmarking heterogeneous electrocatalysts for the oxygen evolution reaction. *J Am Chem Soc*. 2013;135:16977-16987.
55. Indra A, Menezes PW, Sahraie NR, et al. Unification of catalytic water oxidation and oxygen reduction reactions: amorphous beat crystalline cobalt iron oxides. *J Am Chem Soc*. 2014;136:17530-17536.
56. Tiwari JN, Sultan S, Myung CW, et al. Multicomponent electrocatalyst with ultralow Pt loading and high hydrogen evolution activity. *Nat Energy*. 2018;3:773-782.
57. Liu D, Li X, Chen S, et al. Atomically dispersed platinum supported on curved carbon supports for efficient electrocatalytic hydrogen evolution. *Nat Energy*. 2019;4:512-518.
58. Tran PD, Nguyen M, Pramana SS, et al. Copper molybdenum sulfide: a new efficient electrocatalyst for hydrogen production from water. *Energ Environ Sci*. 2012;5:8912-8916.
59. McKone JR, Sadtler BF, Werlang CA, Lewis NS, Gray HB. Ni-Mo nanopowders for efficient electrochemical hydrogen evolution. *ACS Catal*. 2013;3:166-169.
60. Xiao Y, Zhang P, Zhang X, et al. Bimetallic thin film NiCo–$NiCoO_2$@NC as a superior bifunctional electrocatalyst for overall water splitting in alkaline media. *J Mater Chem A*. 2017;5:15901-15912.
61. Huang L, Chen D, Ding Y, Feng S, Wang ZL, Liu M. Nickel-cobalt hydroxide nanosheets coated on $NiCo_2O_4$ nanowires grown on carbon fiber paper for high-performance pseudocapacitors. *Nano Lett*. 2013;13:3135-3139.
62. Corrigan DA. The catalysis of the oxygen evolution reaction by iron impurities in thin film nickel oxide electrodes. *J Electrochem Soc*. 1987;134:377-384.
63. Zeng K, Zhang D. Recent progress in alkaline water electrolysis for hydrogen production and applications. *Prog Energy Combust Sci*. 2010;36:307-326.
64. Zhong ZY, Xiong ZT, Sun LF, et al. Nanosized nickel(or cobalt)/graphite composites for hydrogen storage. *J Phys Chem B*. 2002;106:9507-9513.

SUPPORTING INFORMATION

Additional supporting information may be found online in the Supporting Information section at the end of this article.

How to cite this article: Lu X, Zhang Q, Ng YH, Zhao C. Reversible ternary nickel-cobalt-iron catalysts for intermittent water electrolysis. *EcoMat*. 2020;2:e12012. https://doi.org/10.1002/eom2.12012